ESI for

Turning on the Flexibility of Isoreticular Porous Coordination Frameworks for Drastically Tunable Framework Breathing and Thermal Expansion

Yong-Sheng Wei,[a] Kai-Jie Chen,[a] Pei-Qin Liao,[a] Bao-Yong Zhu,[a,b] Rui-Biao Lin,[a] Hao-Long Zhou,[a] Bao-Ying Wang,[a] Wei Xue,[a] Jie-Peng Zhang[a,*] and Xiao-Ming Chen[a]

[a] MOE Key Laboratory of Bioinorganic and Synthetic Chemistry, State Key Laboratory of Optoelectronic Materials and Technologies, School of Chemistry and Chemical Engineering, Sun Yat-Sen University, Guangzhou 510275, China.

[b] Department of Chemistry, Dezhou University, Dezhou 253023, China.

[*] E-mail: zhangjp7@mail.sysu.edu.cn.

Experimental Section

Materials and Physical Measurements. The organic ligands were synthesized according to the literature.[38, 42, 51] Commercially available reagents and solvents were used as received without further purification. Elemental analyses (C, H, N) were performed on a Vario EL elemental analyzer. Thermogravimetry analyses (TGA) were performed using a TA Q50 instrument from room temperature to 800 °C at a rate of 5.0 °C/min under N_2 flow. Powder X-ray diffraction patterns were recorded on a Bruker D8 ADVANCE or a Rigaku D-MAX 2200 VPC X-ray powder diffractometer (Cu Kα) at room temperature. Gas sorption isotherms were measured on a Micromeritics ASAP 2020M instrument. Magnetic measurements were carried out using a Quantum Design SQUID magnetometer MPMS XL-7.

Synthesis. $[Co_3(\mu_3\text{-OH})(L1)_3]$ (**1-Co**),[36] $[Ni_3(\mu_3\text{-OH})(L1)_3]$ (**1-Ni**),[37] $[Fe_3(\mu_3\text{-OH})(L2)_3]$·guest (**2-Fe·g**),[38] and $[Ni_3(\mu_3\text{-OH})(L2)_3]$·guest (**2-Ni·g**)[38] were synthesized according to the literature.

$[Co_3(\mu_3\text{-OH})(L2)_3]$·guest (2-Co·g). A mixture of $Co(NO_3)_2{\cdot}6H_2O$ (0.029 g, 0.1 mmol), H_2L2 (0.032 g, 0.1 mmol), HBF_4 (0.02 mL), and *N,N*-dimethylacetamide (DMA, 4.0 mL) was stirred for 30 min in air, then transferred and sealed in a 13-mL Teflon-lined stainless container, which was heated in an oven at 130 °C for 3 d, and then cooled to room temperature at a rate of 5 °C h^{-1}, giving purple crystals ca. 0.070 g (60 % yield based on Co).

$[Ni_3(\mu_3\text{-OH})(L3)_3]$·guest (3-Ni·g). A methanol (1.5 mL) solution of NaOH (0.020 g, 0.5 mmol) was added into an *N,N*-dimethylformamide (DMF, 8.0 mL) solution of $Ni(NO_3)_2{\cdot}6H_2O$ (0.029 g, 0.1 mmol) and H_2L3 (0.040 g, 0.1 mmol). After stirred for 1 h, the green suspension was then transferred into a 13-mL Teflon-lined stainless container and kept at 160 °C for 3 d, and then cooled to room temperature at a rate of 5 $^oC{\cdot}h^{-1}$, giving green crystals ca. 0.025 g (20% yield based on Ni). By using DMA instead of DMF, the crystal size is small but the yield is high (70%). When **3-Ni·g** was heated at 150 ^oC in N_2 flow for 30 min, the guest-free phase $[Ni_3(\mu_3\text{-OH})(L3)_3]$ (**3-Ni**) was obtained. Elemental analyses calcd (%) for **3-Ni** ($C_{72}H_{42}N_6Ni_3O_{13}$): C 62.88, H 3.08, N 6.11. Found: C 62.81, H 3.02, N 6.12.

Solvent Exchange. The as-synthesized microcrystalline samples were immersed in corresponding solvents for 4~5 days, during which the solvent was refreshed three times a day.

Single-Crystal X-ray Diffraction Analyses.

All diffraction data used for determination of temperature dependent unit-cell parameters and single-crystal structural analyses were collected using a Bruker Apex CCD area-detector diffractometer (Mo Kα). All single crystal specimens were sealed in glass capillaries, either in vacuum or with minimum amount of corresponding solvent. The measurement temperatures were controlled by a dry nitrogen open flow using a Rigaku Gas Flow GN2 apparatus with temperature fluctuation less than 0.1 K, and corrected by a thermal couple at the crystal position. In the quench experiments, the samples (originally at room temperature) were directly put into the cold flow at 119 K. In other experiments, the temperature was changed in a rate of 20 K/min.

All structures were solved by the direct method and refined with the full-matrix least-squares method on F^2 by the SHELXTL software package. All host-framework non-hydrogen atoms were refined anisotropically. Hydrogen atoms were placed geometrically. The PLATON SQUEEZE treatment was applied to as-synthesized **2-Co·g** and **3-Ni·g** because all guest solvent molecules are extremely disordered and cannot be modeled. Only some of the methanol molecules were located and modeled in **3-Ni·MeOH** because they are highly disordered. All DMF molecules were located and modeled (geometrically constrained) in **3-Ni·DMF**. Some pyridine molecules were found to be ordered in **3-Ni·pyridine**, which were included in the structure refinement. Other disordered residue electron peaks in **3-Ni·pyridine** were removed by the PLATON SQUEEZE treatment. Single crystal data are summarized in Table S1.

Pawley Refinement Details.

a) Data collection: The X-ray powder diffraction data for unit-cell refinement were collected on a Bruker D8 Advance with Cu Kα X-ray (40 kV, 40 mA), with a scanning speed of 0.02°/step and 0.6 seconds/step.

b) Indexing: Indexing and Pawley refinement of the PXRD patterns were carried out by using the Reflex module of Material Studio 5.0. The patterns were indexed by the TREOR90 method with the aid of unit-cell parameters from single-crystal data. Pawley refinements were carried out with the cell parameters obtained from indexing in space group *R*-3*c*. Peak profiles, zero-shift, background, and unit-cell parameters were refined simultaneously. The peak profiles were refined by the Pseudo-Voigt function with Berar-Baldinozzi asymmetry correction parameters. The background was refined with a 20th-order polynomial.

Calculation of thermal expansion coefficients.

The linear thermal expansion coefficient α and volumetric thermal expansion coefficient β were calculated by

$$\alpha = \partial f(T)/\partial T \times 1/f(T) \quad \text{or} \quad \beta = \partial f(T)/\partial T \times 1/f(T)$$

where T is temperature, $f(T)$ is temperature-dependent unit-cell parameter of interest, which was fitted by a suitable polynomial

$$f(T) = a_0 + a_1T + a_2T^2 + a_3T^3 + \ldots$$

for complicated profiles (T-c and T-V of **3-Ni·MeOH**), two polynomials were used to fit the low and high temperature regions.

Table S1. Crystallographic Data and Structural Refinements for **2-Co·g**, **3-Ni·g**, **3-Ni**, **3-Ni·MeOH** and **3-Ni·DMF**.

Compound	**3-Ni·g** (SQUEEZE)	**3-Ni**	**3-Ni**	**3-Ni·MeOH**
Formula	$C_{72}H_{42}Ni_3N_6O_{13}$	$C_{72}H_{42}Ni_3N_6O_{13}$	$C_{72}H_{42}Ni_3N_6O_{13}$	$C_{90}H_{115}N_6Ni_3O_{31}$
Formula weight	1376.25	1376.25	1376.25	1953.01
space group	*R*-3*c*	*R*-3*c*	*R*-3*c*	*R*-3*c*
Temperature (K)	150	119	295	119
a (Å)	29.360(4)	29.884(4)	29.870(4)	29.368(2)
c (Å)	20.776(3)	11.8868(14)	12.0337(15)	20.8680(15)
V (Å^3)	15510(4)	9193.1(19)	9298(2)	15586(2)
Z	6	6	6	6
ρ_{calc} (g cm^{-3})	0.884	1.492	1.475	1.248
μ (mm^{-1})	0.584	0.986	0.975	0.614
$R_1{}^a$ ($I > 2\sigma$)	0.0691	0.0786	0.0873	0.0767
$wR_2{}^b$ (all data)	0.1870	0.1938	0.1949	0.2183
S	1.049	1.093	1.120	1.142

$^a R_1 = \Sigma||F_o| - |F_c||/\Sigma|F_o|$. $^b wR_2 = [\Sigma w(F_o^2 - F_c^2)^2/\Sigma w(F_o^2)^2]^{1/2}$.

Table S1. (Continued)

Compound	**3-Ni·MeOH**	**3-Ni·MeOH**
Formula	$C_{90}H_{115}N_6Ni_3O_{31}$	$C_{82}H_{83}N_6Ni_3O_{23}$
Formula weight	1953.01	1696.67
space group	*R*-3*c*	*R*-3*c*
Temperature (K)	119	295
a (Å)	29.368(2)	29.347(2)
c (Å)	20.8680(15)	21.2870(17)
V (Å^3)	15586(2)	15877(2)
Z	6	6
ρ_{calc} (g cm^{-3})	1.248	1.065
μ (mm^{-1})	0.614	0.588
R_1[a] (I > 2σ)	0.0767	0.0727
wR_2[b] (all data)	0.2183	0.2214
S	1.142	1.097

[a] $R_1=\Sigma||F_o| - |F_c||/\Sigma|F_o|$. [b] $wR_2 =[\Sigma w(F_o^2 - F_c^2)^2/\Sigma w(F_o^2)^2]^{1/2}$.

Table S1. (Continued)

Compound	**3-Ni·DMF**	**3-Ni·DMF**	**3-Ni·DMF**
Formula	$C_{108}H_{127}N_{18}Ni_3O_{25}$	$C_{108}H_{127}N_{18}Ni_3O_{25}$	$C_{108}H_{127}N_{18}Ni_3O_{25}$
Formula weight	2253.41	2253.41	2253.41
space group	*R*-3*c*	*R*-3*c*	*R*-3*c*
Temperature (K)	119	295	119 (quenched)
a (Å)	29.106(3)	29.050(2)	29.151(3)
c (Å)	23.417(2)	24.502(2)	23.070(2)
V (Å^3)	17180(3)	17908(2)	16978(3)
Z	6	6	6
ρ_{calc} (g cm^{-3})	1.307	1.254	1.322
μ (mm^{-1})	0.566	0.543	0.572
$R_1{}^a$ (I > 2σ)	0.1111	0.0785	0.1056
$wR_2{}^b$ (all data)	0.3149	0.2405	0.3069
S	1.242	1.051	1.065

Table S1 (Continued)**.**

Compound	**3-Ni·pyridine** (partially SQUEEZE)	**2-Co·g** (SQUEEZE)
Formula	$C_{109.5}H_{80.5}Ni_3N_{13.5}O_{13}$	$C_{57}H_{34}Co_3N_3O_{13}$
Formula weight	1969.50	1145.66
space group	*R*-3*c*	*R*-3*c*
Temperature (K)	150	295
a (Å)	28.548(4)	19.431(1)
c (Å)	26.592(3)	45.631(3)
V (Å^3)	18769(4)	14920(1)
Z	6	6
ρ_{calc} (g cm^{-3})	1.046	0.765
μ (mm^{-1})	0.502	0.530
$R_1{}^a$ (I > 2σ)	0.0979	0.0461
$wR_2{}^b$ (all data)	0.2767	0.1396
S	1.049	1.066

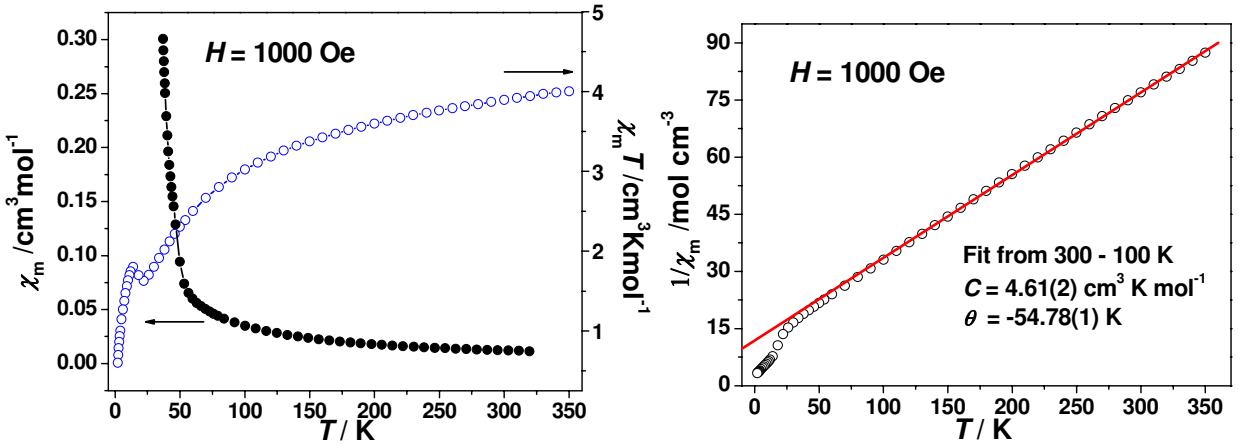

Fig. S1 Temperature dependence of χ_M for guest-free **3-Ni** in an applied dc field of 1000 Oe (left), and fitting with the Curie-Weiss law in the temperature range of 100–300 K (right). The magnetic susceptibility was measured with **3-Ni** contained in gelatin capsules, which was mounted in straw to provide an invariant diamagnetic background that did not influence the SQUID detection coils. DC susceptibility measurement was carried out in applied field of 1000 Oe from 300 K to 2 K. The data was corrected for the diamagnetism from Pascal constants.

In order to confirm the valence of nickel ions, the mangetic susceptibility measurement was performed in an applied field of 1000 Oe for **3-Ni**. The $\chi_M T$ value decreased slowly upon cooling, indicating antiferromagnetic interaction between nickel ions within the trinuclear unit. Fitting the data between 100 and 300 K with Curie-Weiss law gave C = 4.61 cm^3 K mol^{-1}, θ = -54.78 K. The C value is higher than the expected values for 3Ni^{2+}(hs, high spin) (C = 3.0 cm^3 K mol^{-1}) and 2Ni^{2+}(hs) + 1Ni^{3+}(hs) (3.88 cm^3 K mol^{-1}), but lower than that for 1Ni^{2+}(hs) + 2Ni^{3+}(hs) (C = 4.75 cm^3 K mol^{-1}), by assuming g = 2.0 for all ions. However, as well known, Ni^{3+} is a 3d^7 system with $t_{2g}^5e_g^2$ configuration in high-spin state, thus Ni^{3+} usually has a g value larger than 2.0, similar to the high spin Co^{2+} ion, because of a significant spin-orbital coupling interaction. If assuming all nickel ions are Ni^{2+} ions, the g value estimated from the C value is 2.48, much larger than the g value (2.13) that observed in a μ_3-OH bridged trinuclear Ni^{2+} complex (*Russ. Chem. Bull.* 1998, **47**, 1237-1238). Thus, the trinuclear nickel units of **3-Ni** should not consist of three Ni^{2+} ions. For the case of 2Ni^{2+}(hs) + 1Ni^{3+}(hs), the g value estimated from C value is 2.26 for Ni^{3+} using typical value of 2.1 for Ni^{2+}, is reasonable if taking account the spin-orbital coupling effect of nickel ions, and thus, the magnetic susceptibility data support that the trinuclear units in our compounds are consisting of 2Ni^{2+}(hs) ions and 1Ni^{3+}(hs) ion.

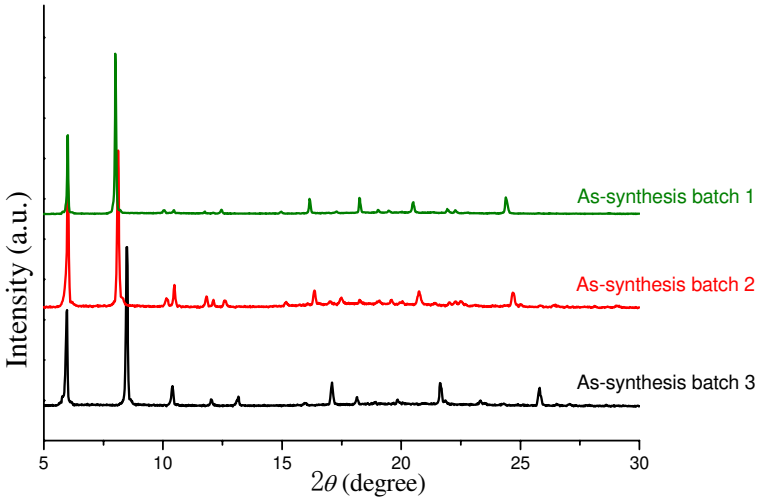

Fig. S2 PXRD patterns of as-synthesis **3-Ni·g** obtained in different batches.

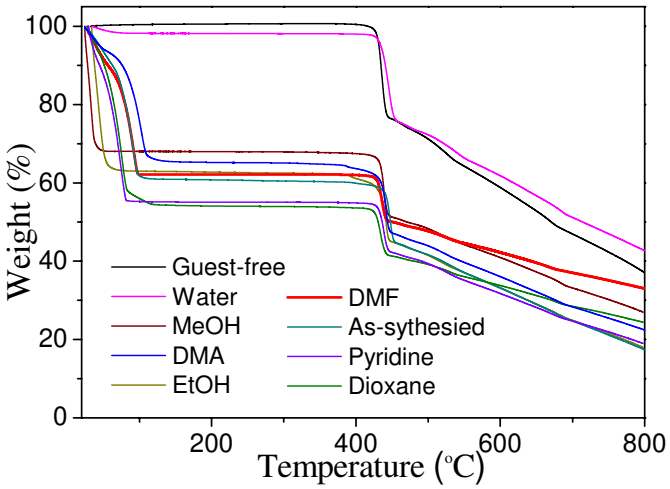

Fig. S3 TG curves of **3-Ni·solvents**, corresponding to inclusion of 1.6 H_2O, 22.5 MeOH, 8.5 DMA, 17.9 EtOH, 11.5 DMF, 14.2 pyridine, and 13.3 1,4-dioxane molecules per formula $[Ni_3(OH)(bpydc)_3]$.

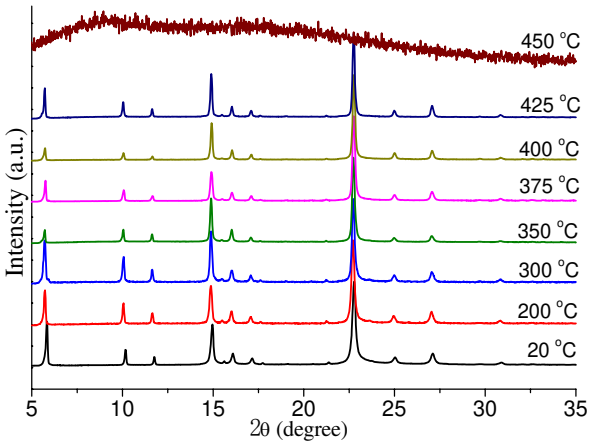

Fig. S4 Room-temperature PXRD patterns of **3-Ni** after heated at different temperatures under N_2 for 20 min.

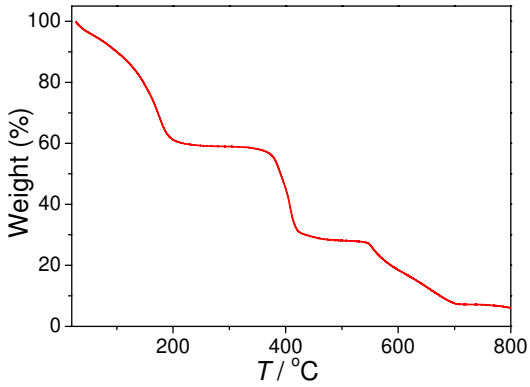

Fig. S5 TG curve of **2-Co·g**.

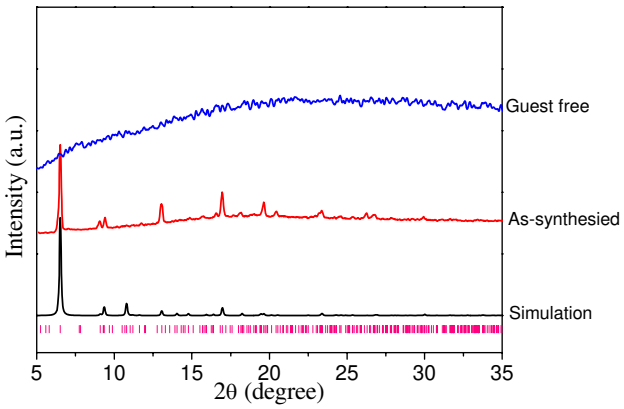

Fig. S6 PXRD patterns for **2-Co·g**.

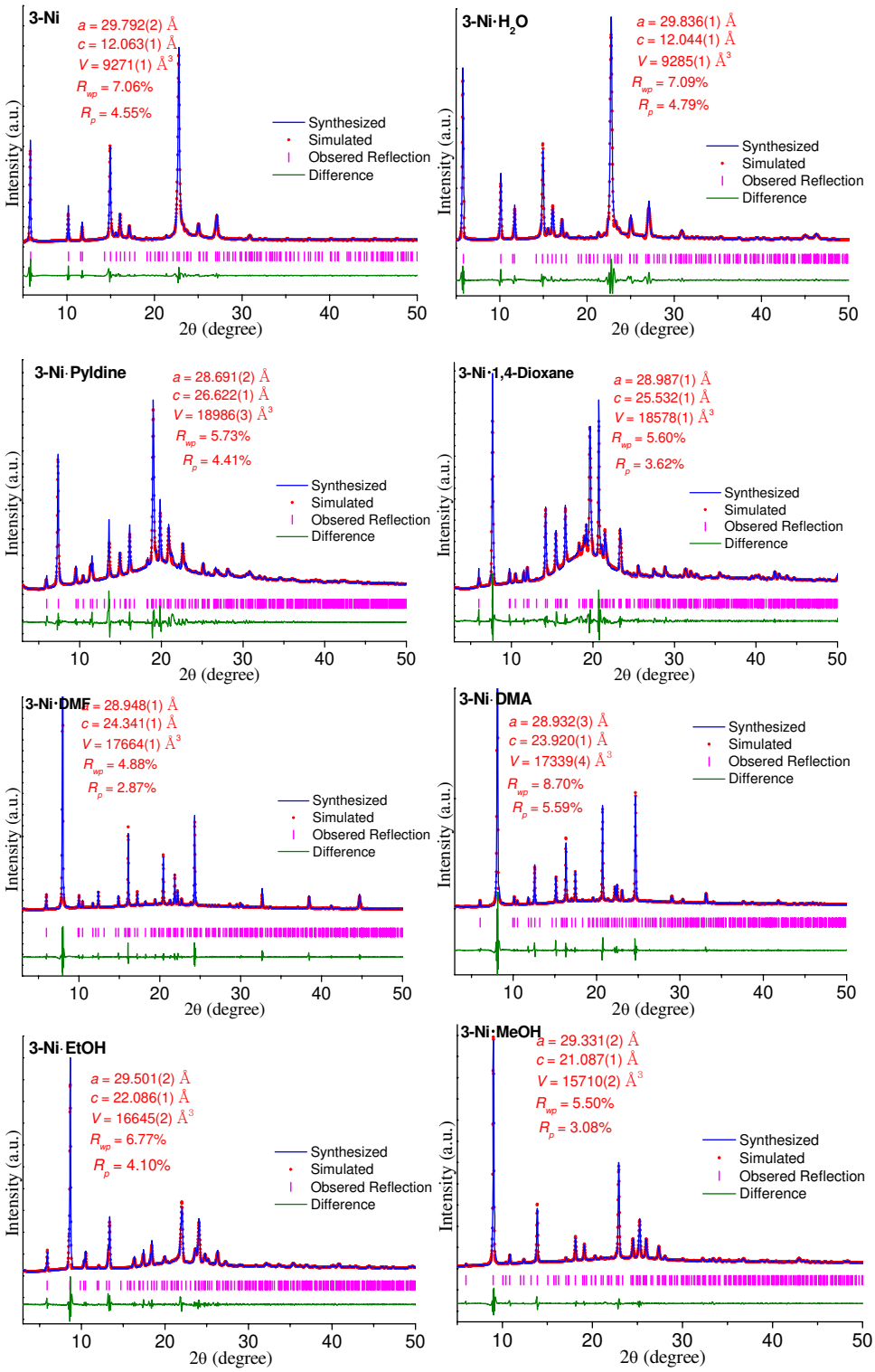

Fig. S7 Pawley refinements of the PXRD patterns for **3-Ni** and **3-Ni·solvents**.

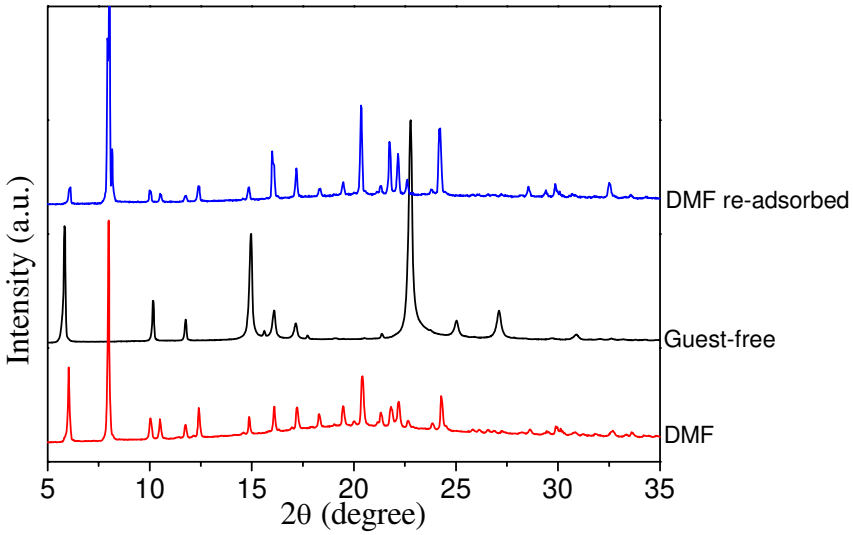

Fig. S8 PXRD patterns of **3-Ni·DMF** after repeated desorption and adsorption.

Table S2. Remarkable guest-induced breathing amplitudes of reported compounds.

Compound	Guest	$\Delta l/l_{min}$ (%)	$\Delta V/V_{min}$ (%)	ref
Ag(I) triazolate (FMOF-1)	N_2	10	10	7
Cu(BDTri)L	DMF	51	40	23
$[CdL_2(ClO_4)_2]$	C_6H_6, EtOH, H_2O	98	101	22
Co(BDP)	N_2	120	140	17, 29
MIL-53	H_2O	40	50	16
MIL-88A	H_2O	50	85	18-19
MIL-88B	MeOH	55	125	18
MIL-88C	Pyridine	80	180	18
MIL-88D	Pyridine	100	230	18
MIL-89	Pyridine	85	160	19
MCF-18(L3,Ni)	MeOH	77	71	This work
MCF-18(L3,Ni)	pyridine	121	105	This work

Note: *l* for axis length, *V* for volume

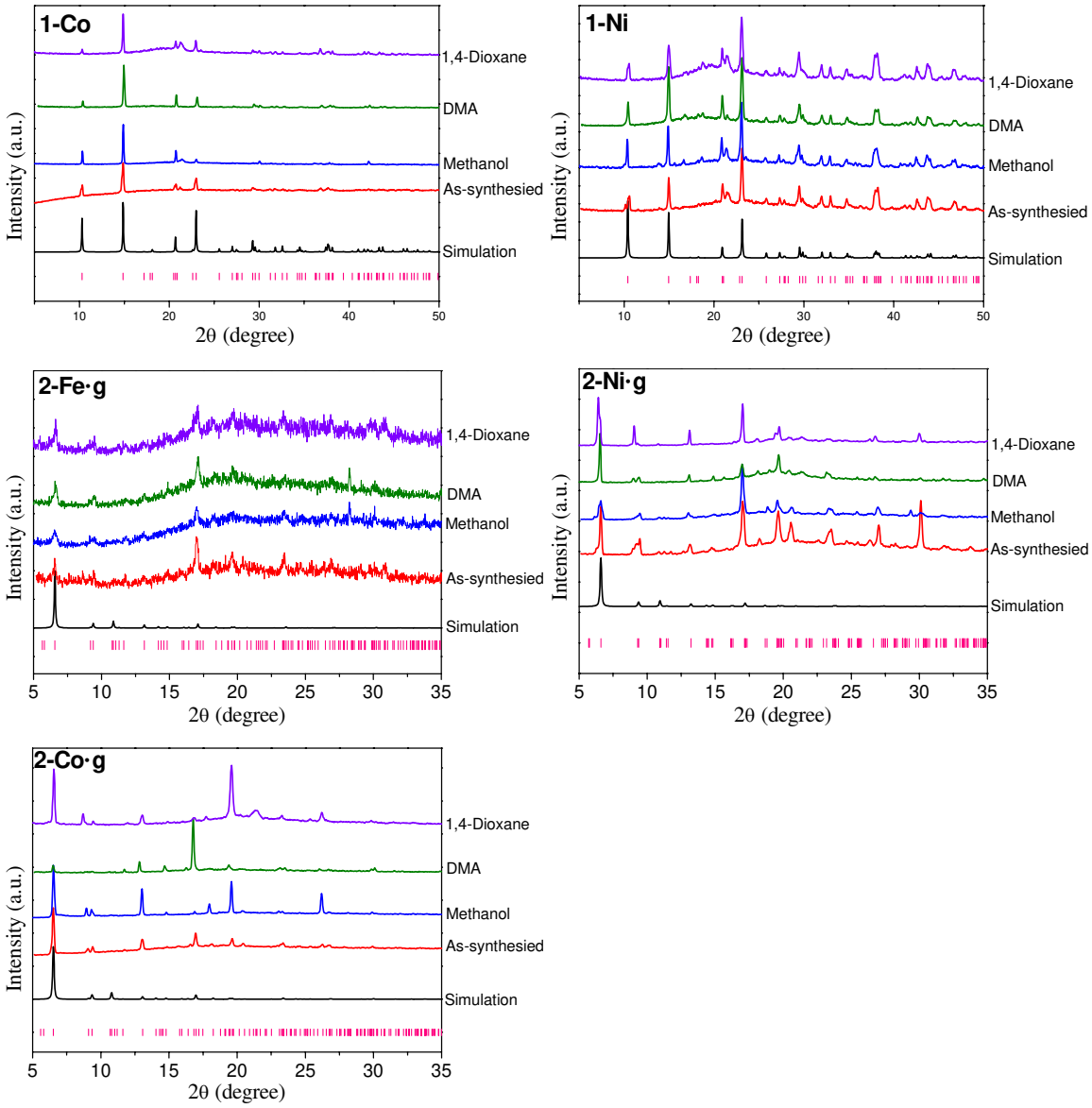

Fig. S9 PXRD patterns of **1-Co**, **1-Ni**, **2-Fe·g**, **2-Ni·g**, and **2-Co·g** after exchange with different solvents. Note that we cannot synthesize high-crystallinity **2-Fe·g**.

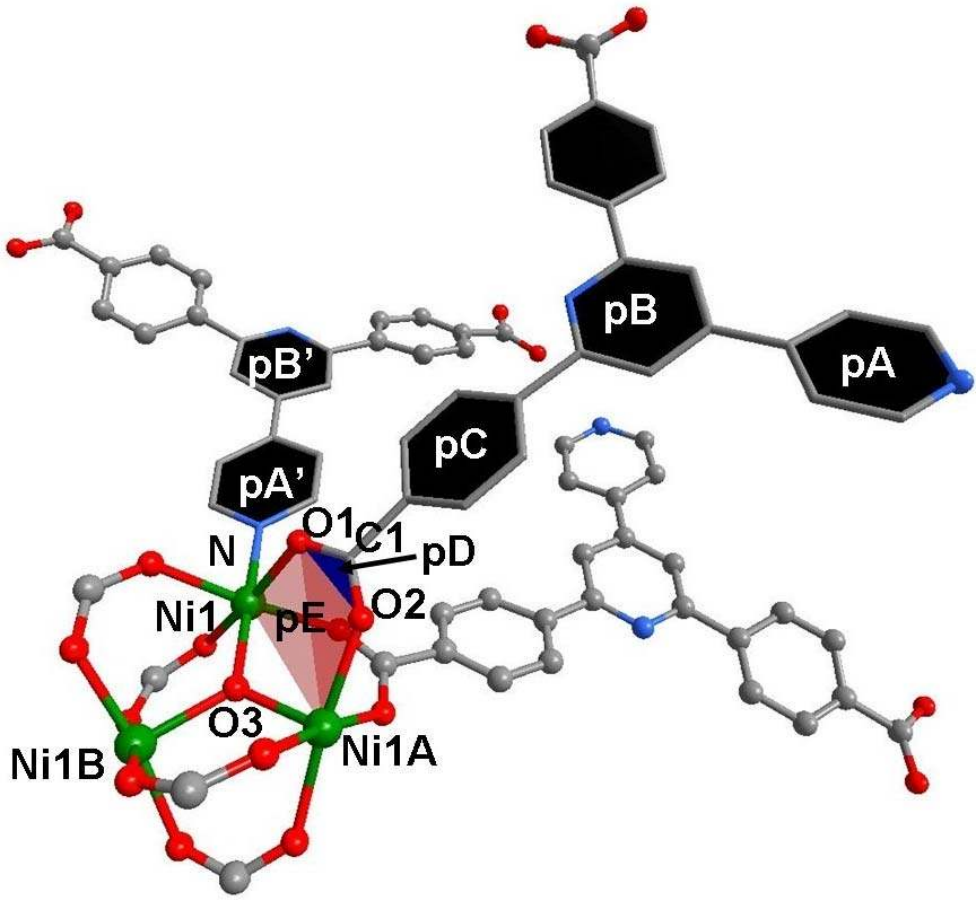

Fig. S10 A representative portion of crystal structures of **3-Ni**, **3-Ni·MeOH**, and **3-Ni·DMF**. Definition of planes: pA (pA' is symmetric equivalent of pA) for coordination pyridyl rings, pB (pB' is symmetric equivalent of pB) for central pyridyl ring, pC for phenyl ring, pD for carboxylate group composed of O1, O2, and C1, pE for Ni_2O_2 plane composed of Ni1, Ni1A, O1, and O2.

Table S3. Comparison of important bond lengths, bond angles, and dihedral angles. Atom and plane numbering see Fig. S10.

Compound	**3-Ni**	**3-Ni·MeOH**	**3-Ni·DMF**	$M_3(\mu_3$-O/OH)$(O_2CR)_6(L^T)_3$
∠Ni-O1-C1 (°)	131.7(4)	124.4(3)	128.3(3)	131.1
∠Ni-O2-C1 (°)	130.1(4)	136.6(3)	134.7(4)	
∠O3-Ni1-O1 (°)	92.9(1)	92.82(8)	94.6(1)	94.8
∠O3-Ni1-O2 (°)	89.8(1)	92.98(8)	93.14(9)	
∠Ni1-O3-Ni1A	119.93(3)-120.07(2)	119.93(2)-120.07(1)	119.93(2)-120.07(1)	119.9
Ni1-O1 (Å)	2.022(5)	2.102(3)	2.073(3)	2.033
Ni1-O2 (Å)	2.107(5)	2.055(4)	2.105(4)	
Ni1-O3 (Å)	2.0610(5)	2.0165(5)	2.0004(3)	1.913
Ni1-N1 (Å)	2.101(3)	2.097(4)	2.084(3)	2.037
O1-C1 (Å)	1.225(8)	1.245(4)	1.248(7)	1.253
O2-C1 (Å)	1.245(5)	1.254(6)	1.252(7)	
∠O3-Ni1-N1	179.9(1)	180	180	177.8
∠Ni1-N1-pA'	0	0	0	/
$\angle Ni_3$-pA'	33.5(1)	9.3(2)/56(1)	2.7(2)	/
$\angle Ni_3$-pB'	1.2(1)	15.9(1)	17.9(1)	/
∠pB-pC (°)	25.7(2)	9.2(2)/23.3(2)	14.7(2)	/
∠pB-pA (°)	34.7(2)	25.2(2)/40.3(1)	15.3(2)	/
∠pC-pD (°)	25.9(3)	22.1(3)	11.0(4)	/
∠pD-pE (°)	34.5(7)	28.7(4)	22.4(4)	~0

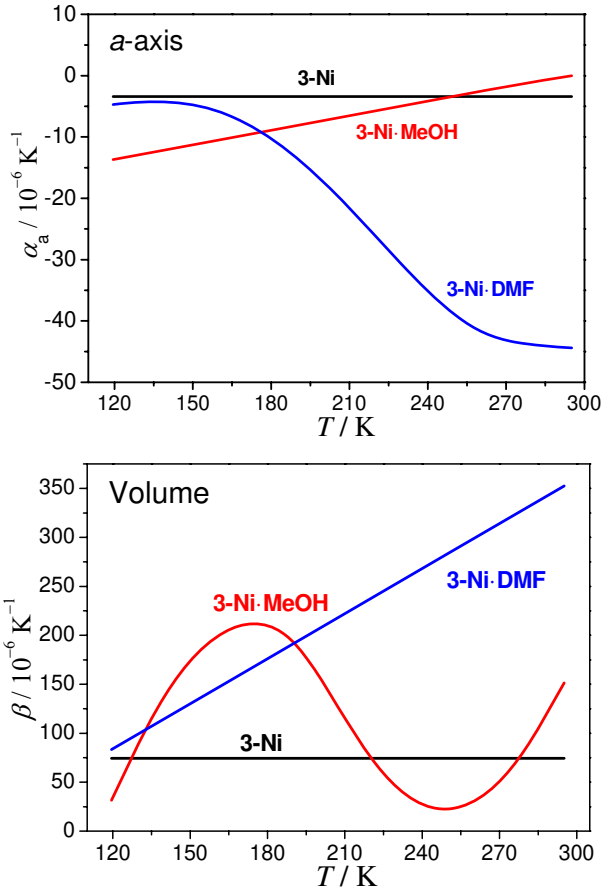

Fig. S11 Temperature dependent thermal expansion coefficients of the unit-cell parameter *a* and *V* for **3-Ni**, **3-Ni·MeOH**, and **3-Ni·DMF**.

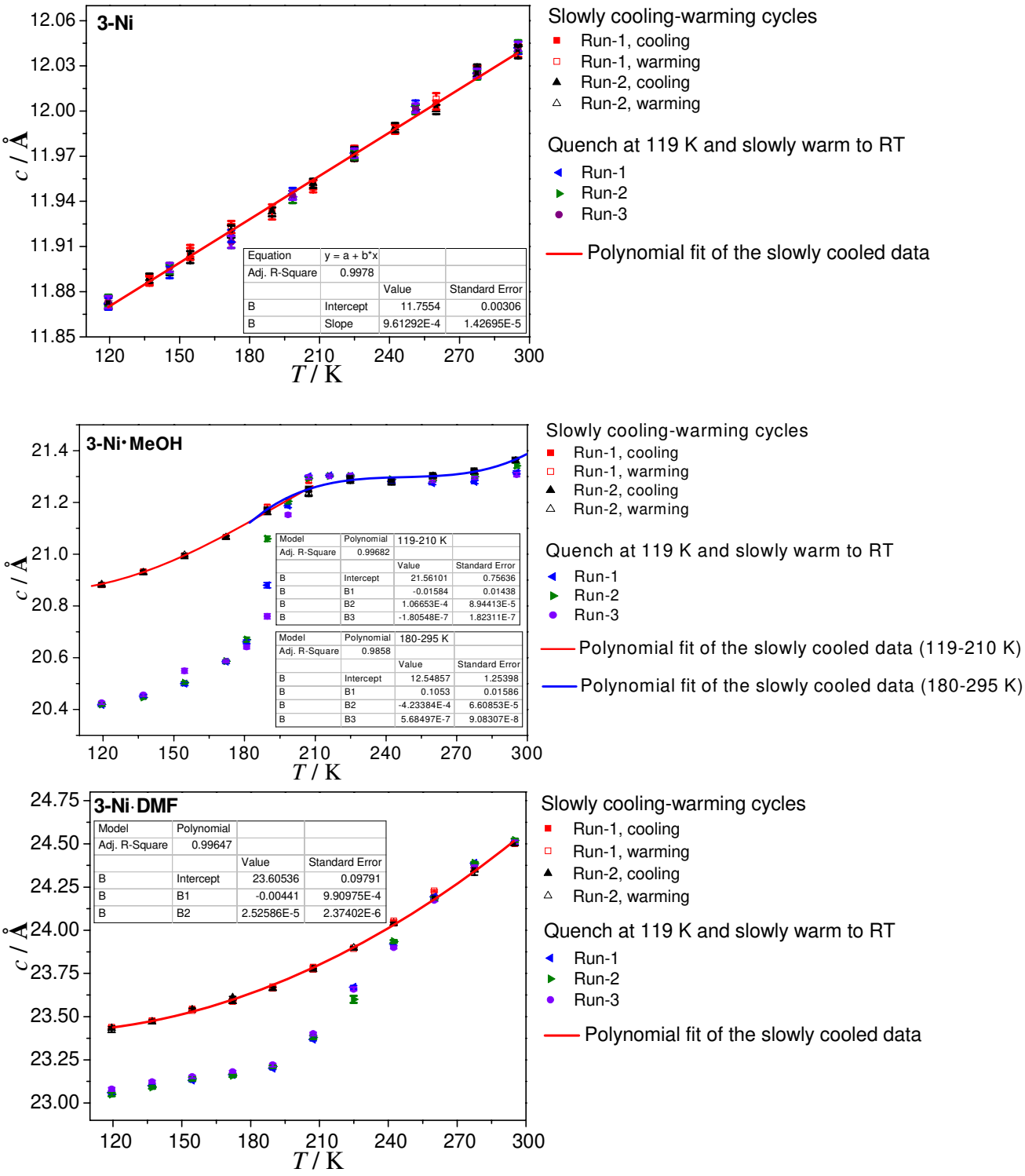

Fig. S12 Repeatability of temperature dependent unit-cell parameter *c* for **3-Ni**, **3-Ni·MeOH**, and **3-Ni·DMF**.

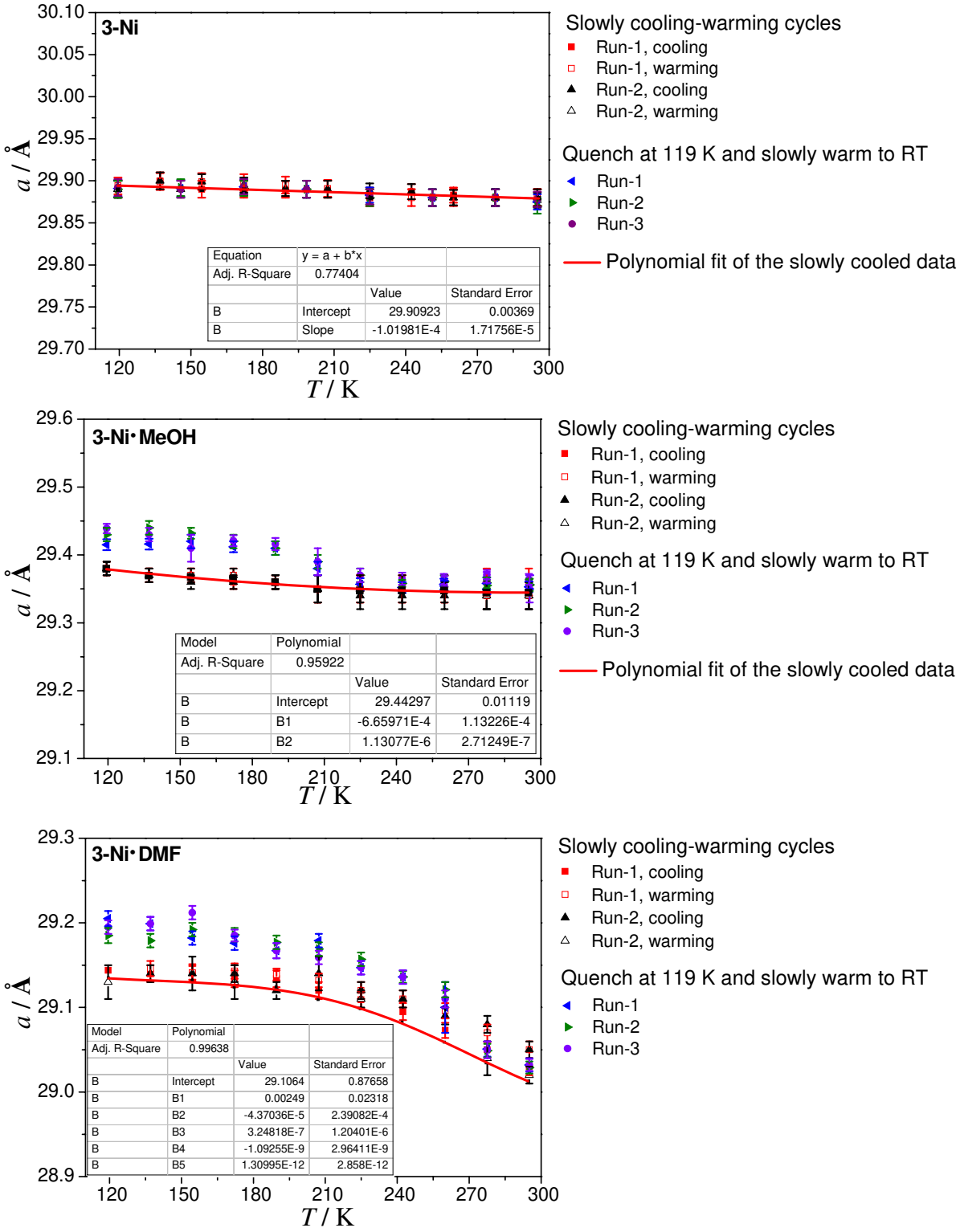

Fig. S13 Repeatability of temperature dependent unit-cell parameter *a* for **3-Ni**, **3-Ni·MeOH**, and **3-Ni·DMF**.

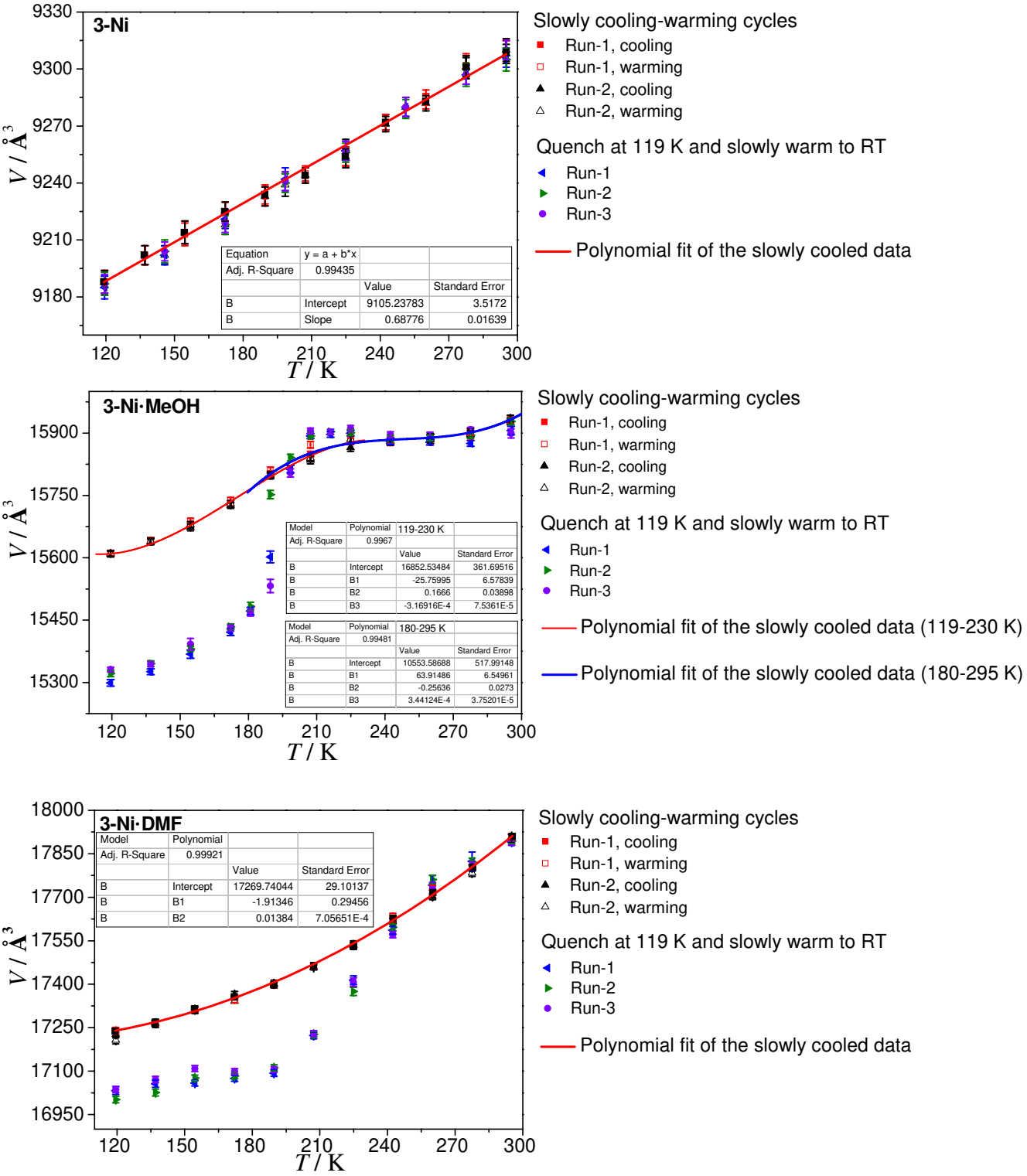

Fig. S14 Repeatability of temperature dependent unit-cell parameter *V* for **3-Ni**, **3-Ni·MeOH**, and **3-Ni·DMF**.

Table S4. Remarkable thermal expansion coefficients of reported compounds.

Compound	α_{max}	β_{max}	ref
ZrW_2O_8	-4.9	-15	1
HKUST-1	-4.1	-12	10
$Cd(CN)_2$	-20.4	-60	6
$Ag_3Co(CN)_6$	150	170	6
HMOF-1	214	163	8
Ag(I) triazolate (FMOF-1)	230	300	7
3-Ni	81 (avg. 81)	74 (avg. 74)	This work
3-Ni·MeOH	242 (avg. 128)	217 (avg. 111)	This work
3-Ni·DMF	437 (avg. 258)	353 (avg. 218)	This work

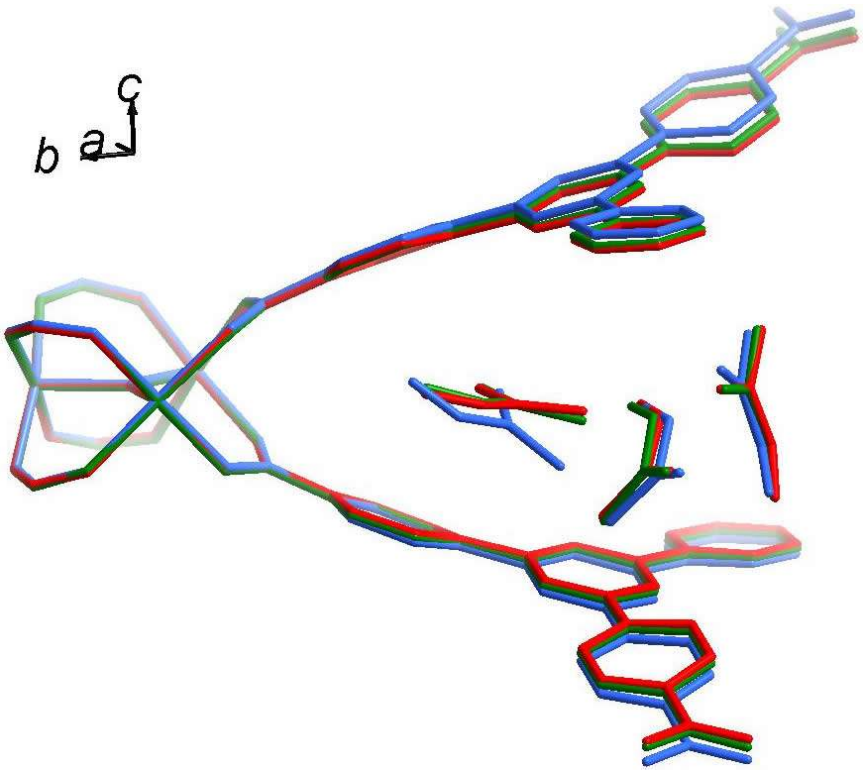

Fig. S15. Structural variations of **3-Ni·DMF** at room temperature (blue), and slowly cooled (green) and quenched (red) to 119 K.